https://doi.org/10.48048/tis.2022.5781

Transient Heat Transfer Analysis on Composite Solids for Hypersonic Flow Applications

Ravi Peetala

Department of Mechanical Engineering, Visvesvaraya National Institute of Technology, Maharashtra 440010, India

(Corresponding author's email: ravipeetala@gmail.com)

Received: 12 July 2021, Revised: 6 August 2021, Accepted: 13 August 2021

Abstract

Surface heating rates have the importance in high speed flow due to viscous or aerodynamic heating which leads to enormous rise in surface temperature. Prediction of exact heat transfer rates is essential for design of protection systems for aerodynamic bodies aimed. For the thermal protection system, the aerodynamic Surfaces are generally configured with multiple solids. Hence present study is planned to develop the conjugate heat transfer (CHT) solver for composite solids. A CHT solver is in hypersonic flow environment. Finite volume framework and explicit time stepping have been implemented for both the compressible Navier-Stokes solver and conduction solver. Loose coupling has been established between the above mentioned fluid and solid domain solvers. The following observations were made in the CHT simulations. In the case of hypersonic flows over finite thickness flat plate, considerable difference in surface heat transfer rate has been noticed along the stream wise direction at the solid-fluid interface and also the Effect of wall material on heat diffusion for hypersonic application has been analyzed using loosely coupled CHT solver. The CHT solver has also been implemented for hypersonic flow over composite cylinder. Necessity of insulating material in the region of stagnation point has been realized as the outcome of these studies.

Keywords: Finite volume method, Hypersonic flow and conjugates heat transfer

Nomenclature

C	Specific heat at constant, kJ/kg-K
E	Total specific energy, kJ/kg
e	Specific internal energy, kJ/kg
H	Total specific enthalpy, kJ/kg
h	Specific enthalpy, kJ/kg
k	Thermal conductivity, W/m-K
L	Length, m
M	Mach number
p	Pressure, N/m^2
$\dot{q}$	Heat flux, W/m^2
Pr	Prandtl number
R	Universal gas constant
Re	Reynolds number
S	Source term
s	Sutherland's constant
S_t	Stanton Number
T	Temperature,ºC
u	X-direction velocity, m/s

Nomenclature

v	Y-direction velocity, m/s
x, y	Cartesian co-ordinate system
FVM	Finite Volume Method
BEM	Boundary Element Method
CHT	Conjugate Heat Transfer

Greek symbols

λ	Courant number
γ	Specific heat ratio
μ	Dynamic viscosity , kg/m-s
τ	Shear stress, N/m^2
ρ	Density, kg/m^3
δ	A parameter in AUSM- δ scheme

Subscripts

∞	Freestream quantities

Introduction

Transient heat transfer analysis is highly essential for the design of engineering objects, such as steam and gas turbines, diesel engine blocks, jet engines, rocket motors, nuclear reactors, etc. It is of significant importance and of scientific relevance to understand the flow in hypersonic applications. High aerodynamic heating rates are associated with high-speed flights and portray even more severe transient heat transfer problems for the design of thermal protection systems for spacecraft and missiles. Design of thermal protection systems (TPS) depends on accurate prediction of the aerothermal loads due to rise in surface temperature. Traditionally, an aerodynamicist predicts the surface pressures and heating rates assuming rigid isothermal boundary at the surface of the vehicle. Such traditional approaches under-predict the interface properties. This analysis is inefficient in high speed and sensitive applications. To overcome the above drawback the present study is focus on conjugate heat transfer analysis (CHT). CHT analysis is considered as a potential means for prediction of heating rates.

From the last 3 decades, various researchers around the globe have performed CHT analysis for estimation of surface properties on the way to design hypersonic flights. Hassan *et al*. [1] presented an iterative loose coupling between a FVM computational fluid dynamics code and a finite element material thermal response code and used it to study the ablation of a re-entry vehicle flying through a ballistic trajectory. Liu *et al*. [2] developed numerical schemes for strongly coupled fluid and solid solver through the constant computation of the heat flux at the fluid-solid interface. The coupled field problem addressed in this paper deals with coupling of convective heat transfer external to the solid body with the conduction heat transfer within the solid body. Thus, conjugate heat transfer applies to any thermal system in which multi-mode convective/conduction heat transfer is of particular importance to thermal design. Hence CHT arises naturally in most instances where external and internal temperature fields are coupled [3-6]. He *et al*. [7,8] adopted the BEM/FVM approach in further studies of CHT in incompressible flow in ducts subjected to constant wall temperature and constant heat flux boundary conditions. Kontinos [9] also adopted the BEM/FVM coupling algorithm to solve the CHT over metallic thermal protection panels at the leading edge of the X-33 in a Mach 15 hypersonic flow regime. Rahim *et al*. [10,11] also used same methodology during development of a CHT solver for transient analysis. Xiaoli *et al*. [12] have introduced a flow-thermal-structural coupling approach based on coupled heat transfer simulation. It is applied to the analysis of a hypersonic aerodynamically heated leading edge, where studies are carried out for Mach number 6.47 flow over a cylinder, for which the flow behaviour and aero-thermal loads are calibrated by experimental data. The numerical results of the surface pressure, cold wall heating rate, hot wall heating rate and temperature distributions are all found well consistent with experimental data. In-

line with these efforts reported in open literature, loosely CHT analysis is planned for the present investigations to initiate the efforts for the conjugate heat transfer analysis for hypersonic flow field.

The hypersonic flow over the object of interest establishes a very strong heat flux field. The regions of high heating rates are leading edge of the plate and stagnation point of the cylinder. Hence heat transfer studies become inevitable to design the heat shield in order to protect the inside pay load for analogous spacecraft configurations. Use of the composite material can be a solution to this problem which may as well reduce the weight of the vehicle. Composite solid domains comprised of insulators like Macor and conductor like aluminium are considered to understand the heat penetration for flat plate and cylindrical geometries. In view of this, a CHT solver is developed and employed for studies of hypersonic flow over composite solids. Finite volume framework and explicit time stepping have been implemented for both the compressible Navier-Stokes fluid flow solver and the solid domain conduction solver. This 2-D fluid flow solver considers AUSM-δ [13] scheme for inviscid flux calculations. Viscous flux computations are carried out using area weighted gradients at the nodes [14]. Loose coupling has been established between the fluid and solid domain solvers [15]. The major objective of the present studies is to understand the effect of composite solid domain on the interface heat flux and temperature using the established CHT solver. Hence these investigations are carried out for finite thickness composite flat plate and cylinder configurations.

Mathematical formulation of CHT studies

The Governing equations for a laminar compressible flow are described by the conservation of mass, momentum, and energy equations. These equations can be written in the conservation form as;

$$\frac{\partial(\rho)}{\partial t}+\frac{\partial(\rho u)}{\partial x}+\frac{\partial(\rho v)}{\partial y}=0 \tag{1}$$

$$\frac{\partial(\rho u)}{\partial t}+\frac{\partial(\rho u^2+p)}{\partial x}+\frac{\partial(\rho v)}{\partial y}=\frac{\partial(\tau_{xx})}{\partial x}+\frac{\partial(\tau_{yx})}{\partial y} \tag{2}$$

$$\frac{\partial(\rho v)}{\partial t}+\frac{\partial(\rho uv)}{\partial x}+\frac{\partial(p+\rho v^2)}{\partial y}=\frac{\partial(\tau_{xy})}{\partial x}+\frac{\partial(\tau_{yy})}{\partial y} \tag{3}$$

$$\frac{\partial(\rho E)}{\partial t}+\frac{\partial(\rho uH)}{\partial x}+\frac{\partial(\rho vH)}{\partial y}=\frac{\partial(u\tau_{xx}+v\tau_{yx}-\dot{q}_x)}{\partial x}+\frac{\partial(u\tau_{yx}+v\tau_{yy}-\dot{q}_y)}{\partial y} \tag{4}$$

The governing equations are reduced to non-dimensional form using following non-dimensional parameters.

$$x=\frac{x^*}{L}, y=\frac{y^*}{L}, u=\frac{u^*}{V_\infty}, v=\frac{v^*}{V_\infty}, \rho=\frac{\rho^*}{\rho_\infty}, p=\frac{p^*}{\rho_\infty {V_\infty}^2},$$

$$T=\frac{T^*}{T_\infty}, E=\frac{E^*}{{V_\infty}^2}, H=\frac{H^*}{{V_\infty}^2}, e=\frac{e^*}{{V_\infty}^2}, h=\frac{h^*}{{V_\infty}^2}$$

$$t=\frac{t^* V_\infty}{L}, \mu=\frac{\mu^*}{\mu_\infty}, q_x=\frac{{q_x}^*}{\rho_\infty {V_\infty}^3}, q_y=\frac{{q_y}^*}{\rho_\infty {V_\infty}^3}$$

Here we are assuming $x, y, u\ldots$ etc. as non-dimensional variables and $x^*, y^*, u^*\ldots$ etc. are the dimensional variables for simplicity. The governing equations in non-dimensional form fluid domain are;

$$\frac{\partial\rho}{\partial t}+\frac{\partial(\rho u)}{\partial x}+\frac{\partial(\rho v)}{\partial y}=0 \tag{5}$$

$$\frac{\partial(\rho u)}{\partial t}+\frac{\partial(\rho u^{2}+p)}{\partial x}+\frac{\partial(\rho uv)}{\partial y}=\frac{\partial(\tau_{xx})}{\partial x}+\frac{\partial(\tau_{yx})}{\partial y} \tag{6}$$

$$\frac{\partial(\rho v)}{\partial t}+\frac{\partial(\rho uv)}{\partial x}+\frac{\partial(\rho v^{2}+p)}{\partial y}=\frac{\partial(\tau_{xy})}{\partial x}+\frac{\partial(\tau_{yy})}{\partial y} \tag{7}$$

$$\frac{\partial(\rho E)}{\partial t}+\frac{\partial(\rho uH)}{\partial x}+\frac{\partial(\rho vH)}{\partial y}=\frac{\partial(u\tau_{xx}+v\tau_{yx}-\dot{q}_{x})}{\partial x}+\frac{\partial(u\tau_{yx}+v\tau_{yy}-\dot{q}_{y})}{\partial y} \tag{8}$$

Where;

$$\tau_{xx}=\frac{1}{\mathrm{Re}_{\infty}}\left\{\lambda\left[\frac{\partial u}{\partial x}+\frac{\partial v}{\partial y}\right]+2\mu\frac{\partial u}{\partial x}\right\} \tag{9}$$

$$\tau_{yy}=\frac{1}{\mathrm{Re}_{\infty}}\left\{\lambda\left[\frac{\partial u}{\partial x}+\frac{\partial v}{\partial y}\right]+2\mu\frac{\partial v}{\partial y}\right\} \tag{10}$$

$$\tau_{xy}=\tau_{yx}=\frac{1}{\mathrm{Re}_{\infty}}\left\{\lambda\left[\frac{\partial u}{\partial y}+\frac{\partial v}{\partial x}\right]\right\} \tag{11}$$

$$\dot{q}_{x}=\frac{-\mu}{(\gamma-1)M_{\infty}^{2}\,\mathrm{Re}_{\infty}\,\mathrm{Pr}}\frac{\partial T}{\partial x} \tag{12}$$

$$\dot{q}_{y}=\frac{-\mu}{(\gamma-1)M_{\infty}^{2}\,\mathrm{Re}_{\infty}\,\mathrm{Pr}}\frac{\partial T}{\partial y} \tag{13}$$

In the above equations from Eqs. (6) - (13), the non-dimensional numbers are, the equation of the state along with the;

$$p=\rho\bar{R}T \quad \text{where} \quad \bar{R}=\frac{1}{\gamma M_{\infty}^{2}} \tag{14}$$

Governing equation for heat transfer analysis alone is the unsteady heat conduction equation which is given as;

$$\rho c\frac{\partial T}{\partial t}=\frac{\partial}{\partial x}\left[k\frac{\partial T}{\partial x}\right]+\frac{\partial}{\partial y}\left[k\frac{\partial T}{\partial y}\right]+S \tag{15}$$

Sutherland's formula is used for viscosity calculation in fluid domain while thermal conductivity of solid is considered as constant. FVM based cell cantered explicit formulation is used for fluid domain computations. Solid domain computations are carried out using technique mentioned by Veersteeg and Malalasekera [16]. Explicit formulation is used for the solid domain and fluid flow using fluid domain based time step calculations. Above mentioned governing equations are used for loosely coupled CHT

analysis to investigate hypersonic flow over a flat plate and cylinder. Fluid flow solver has been validated for hypersonic flow over isothermal flat plate while the heat conduction solver has been verified for unsteady heat conduction problems. In-house heat conduction solver is successfully validated for 2D transient composite heat conduction problem with Pietro and Domenic [15]. Excellent agreement with the literature is found. Then, they are combined for loosely coupled CHT analysis using interface heat flux and temperature boundary conditions. In this methodology, the governing equations for fluid flow and heat conduction are solved simultaneously till the residue of the fluid domain attains a desired value. The maximum temperature in the solid domain is marked at this stage and computations in the fluid domain are terminated. Time marching in the solid domain is continued with the enhanced time step till the maximum temperature of the solid domain attains a user defined value. In the present investigations, this value is taken as 1 % of the marked maximum temperature.

The extensive literature survey for turbine isentropic efficiency and mass flow rate models has been conducted. This section presents the existing models in the available literature.

Computational strategy for flow over a composite flat plate and cylinder

Conjugate heat transfer analysis has been carried out for free stream conditions pertaining to typical test conditions of a shock tunnel [17]. Free stream Mach numbers considered for the present studies are 8 with pressure as 89 N/m^2 while the free stream temperature and the initial wall temperature are taken as 113 K and 300 K, respectively. Insulators (e.g. Macor) and conductor (e.g. aluminium) are chosen in the solid domain (i.e. wall) because they are most commonly used as backing materials for thermal sensors during ground/flight experiments. The properties of the wall materials used in the present investigations are given in **Table 1**. CHT solver is validated with experimental data on flow over cylinder and double wedge problems [18-20]

Table 1 Different materials used for composite solid domain.

Material	**Thermal conductivity** $(k)\ (\mathrm{W/m.K})$	**Density** (ρ) $(\mathrm{kg/m^3})$	**Specific heat** (c_p) $(\mathrm{J/kg.K})$	**Thermal diffusivity** $\alpha = k/(\rho c_p)$ $(\mathrm{m^2/s})$
Macor	1.46	2,520	790	$7.3\times10-7$
Aluminum	204	2,704	896	$8.4\times10-5$

Results and discussions

Flow over a composite flat plate and cylinder are analyzed for finding heat flux and temperature along the surface. The heat penetration rate in various wall materials is studied, at different time scales, using fluid flow solver and CHT solver. The results are discussed in subsequent sections.

Fluid flow study with isothermal and adiabatic boundary

A reference test case has been considered as a first step for proposed CHT analysis using only fluid domain. In this case, compressible fluid flow solver is tested for hypersonic flow over flat plate with stream wise varying boundary conditions as shown in **Figure 1**. Two test cases are performed and the boundary is divided into 2 portions i.e., first half isothermal and second half adiabatic (Case I) and vice versa (Case II) as shown in **Figure 1**. Major reason to perform this test is to get the extreme results. Hence, consideration on part of the wall as isothermal will simulate for the infinite conductivity material in that part while the adiabatic boundary condition will imitate the material to be of zero conductivity. Hence, effect of extreme material properties or wall composition can be understood in these reference cases. Temperature contours shown for such cases are shown in **Figure 2**. In **Figures 2(a) - 2(b)** the leading edge half portion is adiabatic and the downstream half portion is isothermal boundary. It is clearly visible in both the figures that the adiabatic region has higher temperature rise in the vicinity of the wall in comparison with the corresponding ideal conductor (isothermal wall).

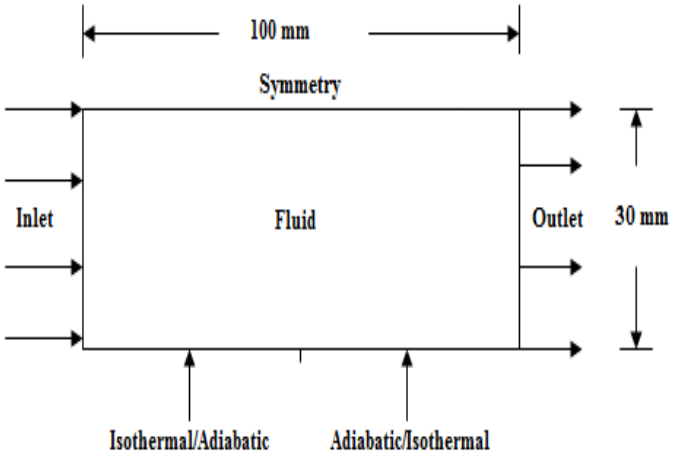

Figure 1 Schematic representation of fluid domain computational geometry for Flat plate.

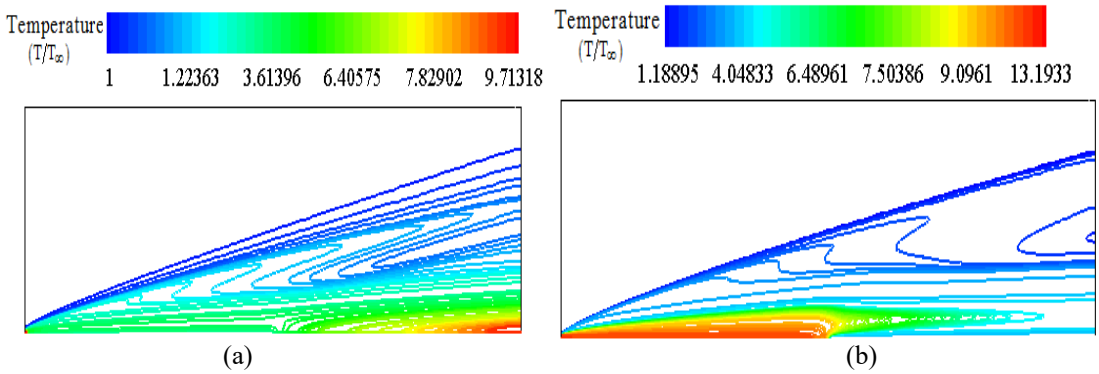

Figure 2 Temperature contours for fluid domain with different BC's at the bottom wall; (a) Case-I (Isothermal-Adiabatic), and (b) Case-II (Adiabatic-Isothermal).

CHT analysis for flow over a composite flat plate

The fluid flow solver (N-S solver) is initially employed for the isothermal wall boundary at the first half and adiabatic wall boundary at the other half of the wall and vice versa. These results are compared with that of the results obtained for the different materials used here in CHT analysis to analyze the effect of composite domain. Computational domain shown in **Figure 3** has been considered for present CHT investigations. The composite solid domain analysis has 2 materials of different thermal conductivities. The effect on the variation of temperature at the surface of the solid is also of present interest. Apart from this, these simulations are also useful to understand the effect of heat interaction on fluid domain with various permutations of wall materials. Therefore, the wall materials viz. aluminum and Macor are chosen since these real materials have large difference in high conductivities. These composite CHT studies are carried out for 2 test cases as given below;

a) Leading edge half portion as aluminium and trailing edge half as Macor.

b) Leading edge half portion as Macor and trailing edge half as aluminium.

These results are compared with the fluid flow solver results for isothermal-adiabatic boundary conditions. Such CHT studies are carried out for simulation duration of 0.1, 0.5 and 1 s. The surface heat flux variation at the fluid-solid interface in the normalized form using freestream parameters, expressed as Stanton number as;

$$s_t = \frac{q_t}{\left\{\rho_\infty u_\infty [C_p (T_0 - T_w)]\right\}} \tag{16}$$

The variation of Stanton numbers along the length of the plate using fluid flow solver. As seen in **Figure 4(a)**, Stanton number decrement along the length of the plate as observed in isothermal-adiabatic combination (case I) is in well agreement with the case-a. Marginal decrease, in leading edge Stanton number has been noticed when aluminium material is used in composite CHT studies at the leading edge. Such leading edge decrease of heat flux is attributed to the strong stream wise heat flux gradient and high thermal conductivity of Aluminium. Similarly, variation of Stanton number along the length of the plate is seen (**Figure 4(b)**) with Macor as leading edge material.

Temperature variation along the solid-fluid interface is plotted for both the cases in **Figures 5** and **6**. The comparison of case-I of fluid flow solver and case-a of CHT simulations for temperature variation (**Figure 5**) show temperature rise of 7 K at higher CHT simulation time of 1 s. There is a sudden change in temperature at the solid-solid interface in CHT simulation and fluid flow solver as well. As the CHT simulation time increases, temperature rise increases which is noticed to be around 700 K for fluid flow solver. It is due to lesser heat penetration for the trailing half due to an insulating material (Macor). Similarly, for the second test case (case-II and case-b), temperature variation along the solid-fluid interface is plotted for both the cases (**Figure 6**). Results obtained from fluid flow solver with adiabatic wall boundary at the first half and isothermal wall boundary at the other half are compared with CHT simulation (Macor-aluminium) in this figure. As the CHT simulation time increases, temperature raise increases at all locations which are marginal at the interface. Near the leading edge, temperature is higher with increase at around 500 K for 1s CHT simulation time. For the first half, fluid flow solver (i.e. adiabatic wall boundary) based temperature rise is noticed to be more around 1,750 K. The major reason for such increase is the presence of insulating wall boundary condition at the leading edge which when replaced by Macor in case of the CHT simulation shown around 500 K at 1 s. There is a sudden decrease in temperature at the solid-solid interface in CHT simulation and fluid flow solver (adiabatic-isothermal) at the interface for this case as well.

At this interface location, the temperature obtained from the fluid flow solver decreases suddenly as the boundary condition changes from adiabatic to isothermal one. In the second half portion of the plate, material used is high conductivity material (Aluminium) in CHT simulation. Therefore, heat penetration is much faster inside the solid as compared to the Macor portion and hence surface temperature rise is less as shown in **Figure 6**. Typical temperature contours for fluid and solid domains corresponding to 1 s are shown in **Figure 7** and **8**. In both the cases for finite thickness flat plate, the maximum temperature rise in the solid domain is noticed at the Macor side. The low thermal conductivity of Macor material does not allow the heat to penetrate into the solid domain hence the temperature rise is more at the surface as compared to the aluminium side where heat penetration is more and hence temperature rise at the surface is less as seen in **Figures 5** and **6**. Temperature and Velocity profiles at 2 selected locations are plotted in **Figures 9** and **10** respectively. These figures basically accommodate the case-I and II along with case-a and case-b. Fluid properties change with the change in wall temperature at location x = 0.025 m and location x = 0.075 m from the leading edge is shown in **Figure 9**. At x = 0.025 m location, the changes are less because wall temperature rise is less compared to the case II (adiabatic-isothermal). Here, as expected, a slightly higher temperature rise is observed for the Macor material at the leading edge compared to the aluminium at the leading edge. At location x = 0.075 m from the leading edge, the temperature rise not only depends on the wall material and boundary but it will also be affected by the heat diffusion from the preceding section of flow field. Here, for the extreme case of isothermal-adiabatic material (case I), the temperature rise is significant due to adiabatic boundary at this location. Whereas in the opposite case (case II), although there is an isothermal boundary at the location, the temperature rise is higher. This is due to the diffusion of heat from the flow field prior to it at the adiabatic boundary. For the other 2 cases the temperature rise is not so appreciable and is comparable. Similarly, velocity changes are noticed in **Figure 10**. Changes in the fluid domain with change in wall conditions are clearly evident from these figures.

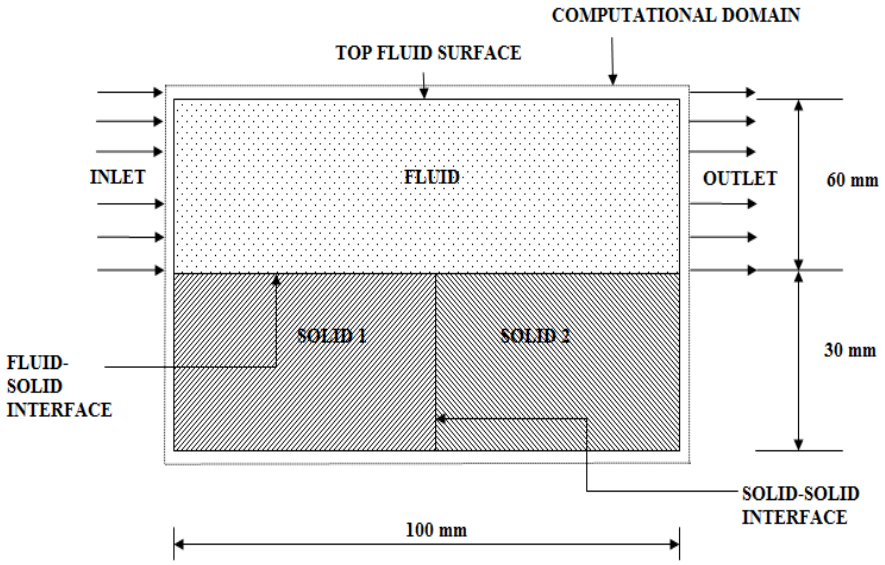

Figure 3 Computational domain for the composite flat plate CHT analysis.

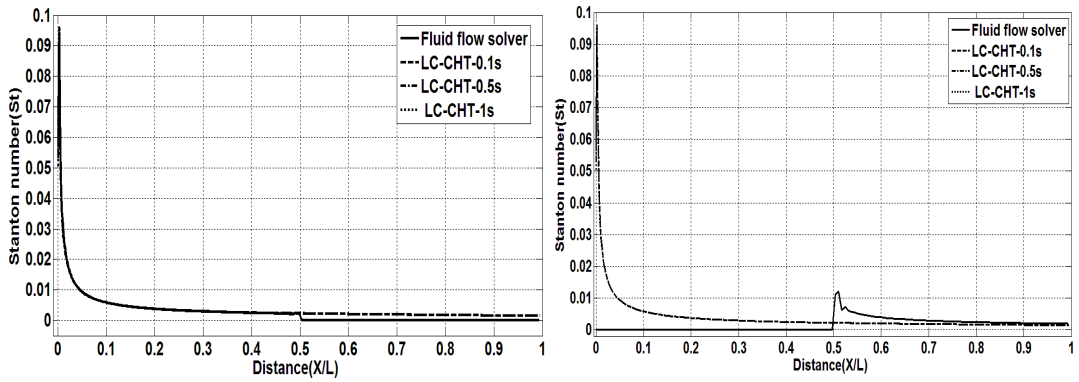

Figure 4 Surface heat flux variation along the length of the flat plate; (a) Aluminium- Macor, and (b) Macor- Aluminium.

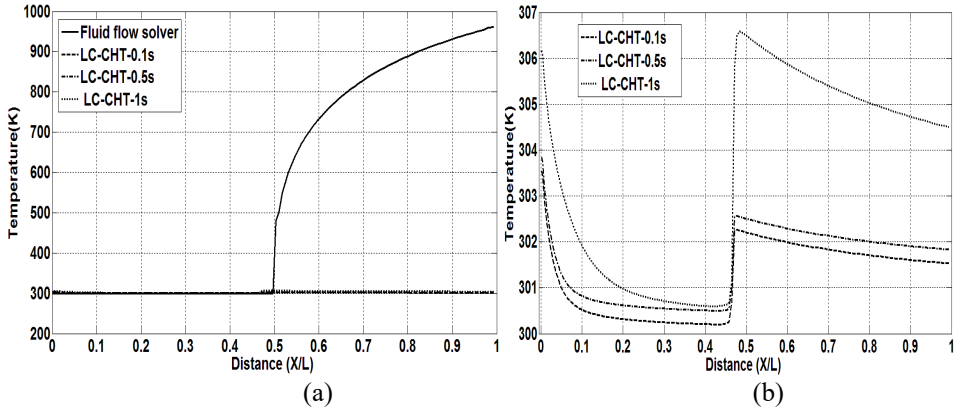

Figure 5 Temperature variation along the length of the flat plate (Aluminium-Macor); (a) Comparison of surface temperature with fluid flow solver, and (b) Surface temperature rise in CHT.

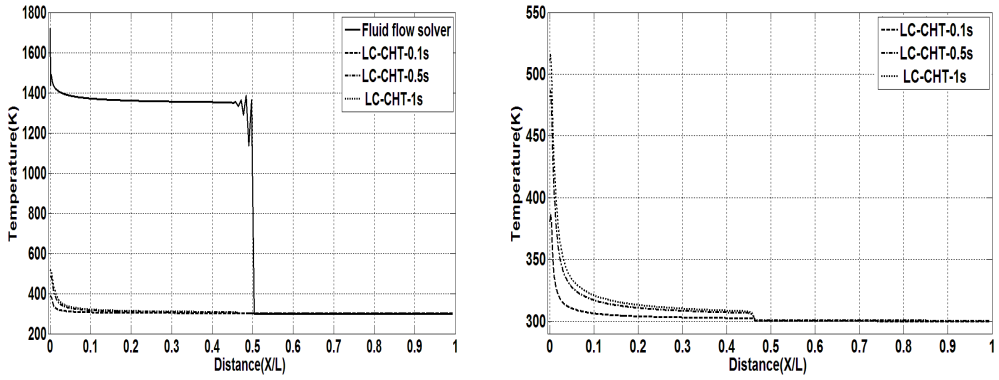

Figure 6 Temperature variation along the length of the flat plate (Macor- Aluminium); (a) Comparison of surface temperature with fluid flow solver (N-S solver), and (b) Surface temperature rise in CHT.

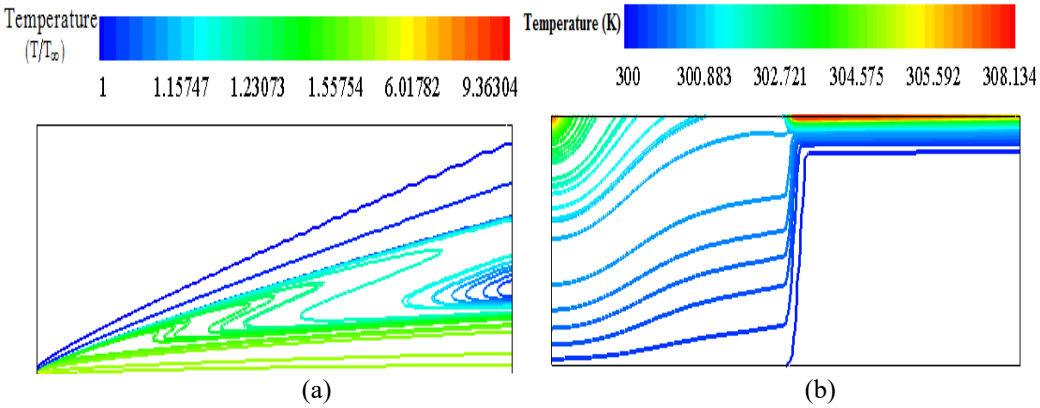

Figure 7 Temperature contour for flat plate fluid and solid domain for case-a; (a) Fluid domain, and (b) Solid domain (Aluminium-Macor).

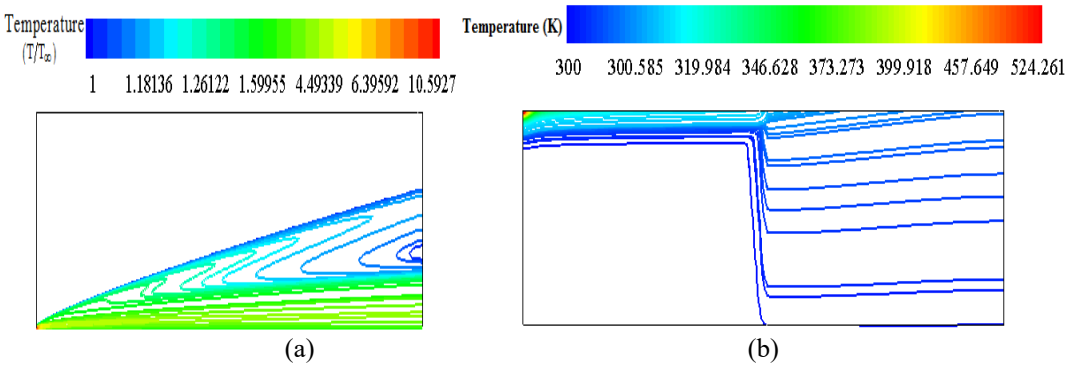

Figure 8 Temperature contour for flat plate fluid and solid domain for case-b; (a) Fluid domain, and (b) Solid domain (Macor-Aluminium).

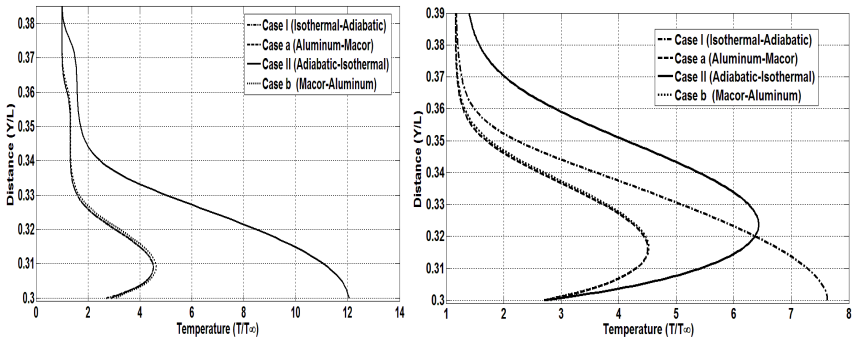

Figure 9 Temperature profile at various locations using all the methods. (a) at x = 0.025 m, and (b) x = 0.075 m.

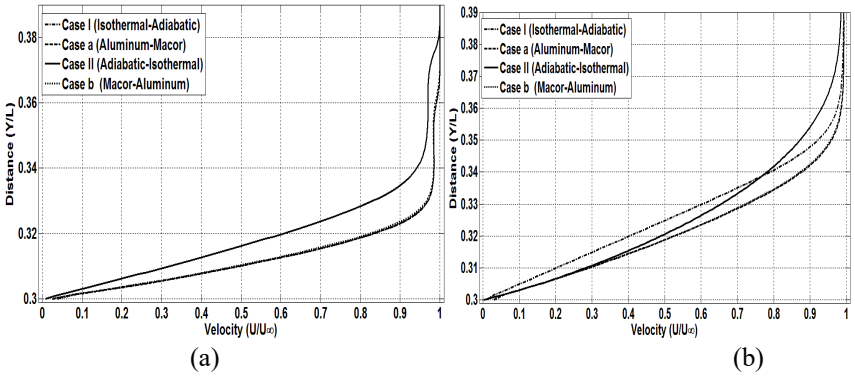

Figure 10 Velocity profile at various locations using all the methods. (a) x = 0.025 m, and (b) x = 0.075 m.

CHT analysis for flow over a composite cylinder

The composite cylindrical domain considered for CHT simulations is as shown in **Figure 11**. The free stream Mach numbers considered for the present studies are 8 with pressure as 89 N/m^2 while the free stream temperature and the initial wall temperature are taken as 113 and 300 K, respectively. Again, same 2 materials and their location based permutations are considered for this case. Hence here as well flow will encounter the change in wall material in the streamwise direction. The Stanton number and temperature variation is shown along the fluid-solid interface in **Figures 12** and **13** respectively. At the first half portion of cylinder, aluminium is used as the high conductivity material and at the second half portion of the cylinder, Macor is used as the insulating material for which results are shown in **Figures 12(a)** and **13(a)**. Stanton number decreases along the fluid-solid interface. In CHT analysis, no significant change in surface heat flux is observed in this figure near the stagnation region where aluminium is present. However, small decrement in Stanton number with simulation time increases (**Figure12(a)**) is noticed in the downstream Macor portion. Again, CHT simulations are carried out with the first half portion of solid material as Macor and second half portion of the solid material as aluminium. As the CHT simulation time increases Stanton number decreases in the first half portion as shown in **Figure 12(b)**. Similarly, here as well, no significant change in Stanton number is noticed in the downstream aluminium part. Hence these figures clearly portray that the presence of Macor decreases the wall heat flux with time. The reason for this is clear in **Figure 13** which displays surface temperature variation with time. The maximum temperature for aluminium increases from 300.5 K at the solid-solid interface at 0.1 s to 306.5 K at 1 s due to higher thermal diffusivity of aluminium (as shown in **Figure 13(a)**). However, the maximum temperature for Macor increases from 315 K at the solid-solid interface at 0.1 s to 360 K at 1s due to lower thermal diffusivity of Macor (as shown in **Figure 13(b)**). Hence, although aluminium has faced stagnation point high heat flux, the temperature rise is only 6.2 K in 1 s. But the Macor portion shows around 60 K raise in temperature in the same duration for 8 % lesser heat flux. Thus, increase in wall temperature is though prominent in CHT, it is more significant in Macor portion. This fact can be cross verified when Macor is present in the stagnation region. In this case, as per **Figure 13(b)**, stagnation

point temperature rise is 80 K where maximum temperature in the aluminium region is hardly 6 K at 1 s.

The heat penetration in solid and fluid domain and associated temperature variations are shown in **Figures 14** and **15** respectively. For the fluid domain, at the stagnation point, kinetic energy is converted into heat energy due to which high temperature fluid is present in the stagnation region as observed in both the figures. Hence higher heat transfer rates are expected and observed (**Figure 14**) in the vicinity of stagnation region. The temperature contour shows the high temperature area for the material with low conductivity material i.e. Macor. There is a larger penetration of heat on the other side as a higher thermal conductive material used (i.e. Aluminium). Thus, use of insulating material in the stagnation region does not allow heat penetration inside the solid. However, presence of heat conducting material in this region thermally disturbs the solid domain. In view of this, CHT studies are essential to predict the depth of heat penetration and effect of wall material on fluid domain in designing the thermal protection system.

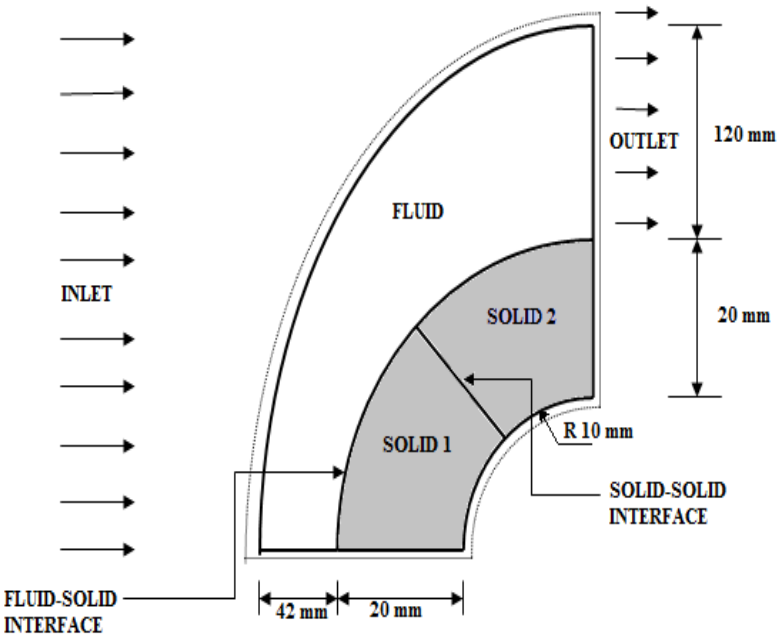

Figure 11 Computational domain for the composite cylinder CHT analysis.

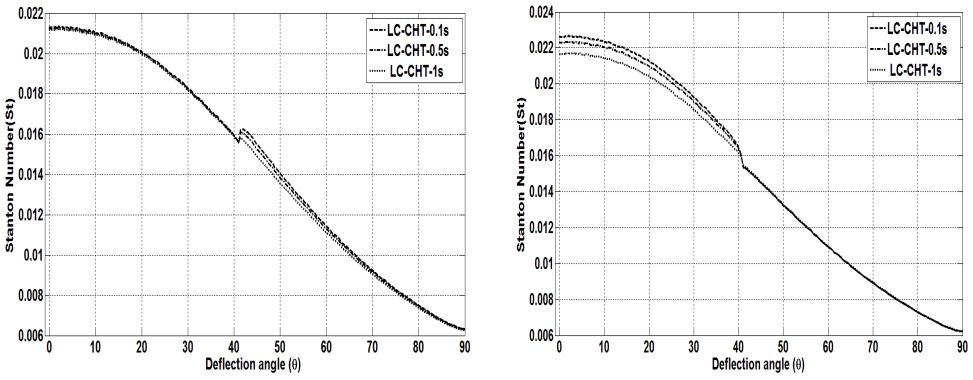

Figure 12 Surface heat flux variation along the surface of the cylinder; (a) Aluminium-Macor, and (b) Macor-Aluminium.

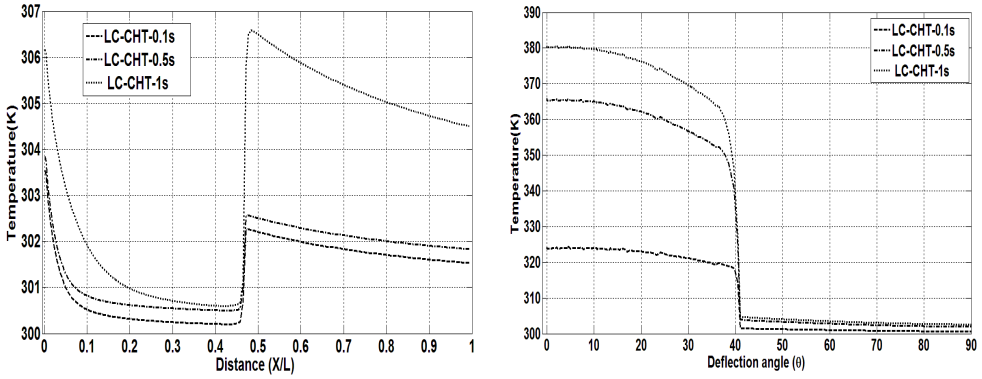

Figure 13 Temperature variation along the surface of the cylinder; (a) Aluminium-Macor, and (b) Macor-Aluminium.

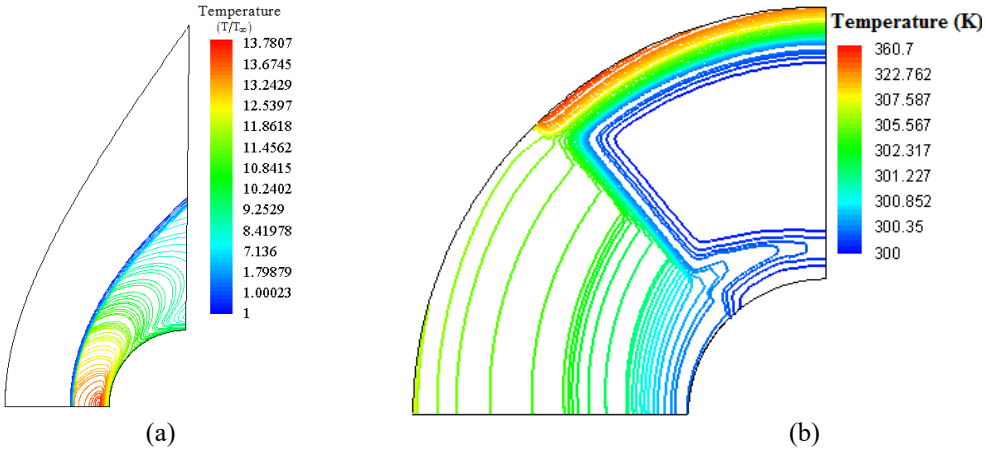

Figure 14 Temperature contour for cylindrical fluid and solid domain for case-I; (a) Fluid domain, and (b) Solid domain (solid1-Aluminum, solid2-Macor).

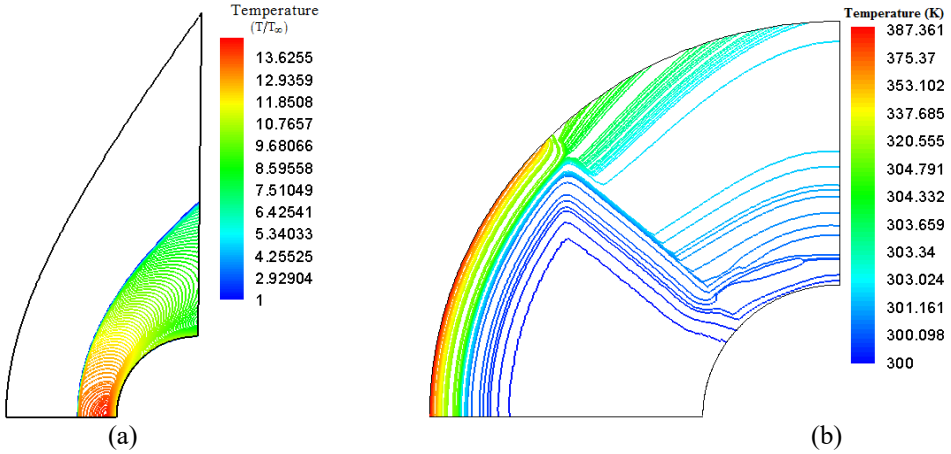

Figure 15 Temperature contour for cylindrical fluid and solid domain for case-II; (a) Fluid domain, and (b) Solid domain (solid1-Macor, solid2- Aluminium).

Conclusions

Successfully implemented CHT analysis for composite solids, since thermal protection systems are generally configured with multiple solids. It has been noticed that the composite CHT studies are useful for the design of thermal protection systems for hypersonic vehicles. 1) It is observed that when insulating material is used in solid domain, the heat penetration and the magnitude of temperature rise is very less within the solid domain and is limited to the surface only. The surface temperature rise is very high for the low thermal conductivity material and it reaches the stagnation temperature at a much faster rate. 2) The high thermal conductivity material there is a larger depth of penetration of heat inside the solid domain and the surface temperature rise is comparatively very less. 3) The idea of using lower conductivity material at the leading edge and other such regions where there is higher heat flux generation will prominently help in thermal protection of vehicles. Thus, solvers can be useful for the design of thermal protection systems for hypersonic vehicles.

References

[1] B Hassan, D Kuntz and DL Potter. Coupled fluid/thermal prediction of ablating hypersonic vehicle. *In*: Proceedings of the 36th AIAA Aerospace Sciences Meeting and Exhibit, Nevada. 1998.

[2] AJ Kassab and MH Aliabadi. *Advances in boundary elements: Coupled field problems*. Computational Mechanics, Massachusetts, 2001.

[3] L Fung-Bao. A modified genetic algorithm for solving the inverse heat transfer problem of estimating plan heat source. *Int. J. Heat Mass Tran*. 2008; **51**, 3745-52.

[4] L Hongpeng and W Zhenguo. Fluid-thermal-structural coupling investigations of opposing jet in hypersonic flows, *Int. J. Heat Mass Tran*. 2021; **120**, 105017.

[5] M Yu-Shan, L Yan, W Huang and W Zhong-Wei. Fluid-thermal coupled investigation on the combinational spike and opposing/lateral jet in hypersonic flows. *Acta Astronautica* 2021; **185**, 264-82.

[6] D Zhou, Z Lu, T Guo and G Chen. A loosely-coupled gas-kinetic BGK scheme for conjugate heat transfer in hypersonic flows. *Int. J. Heat Mass Tran*. 2020; **147**, 119016.

[7] M He, PJ Bishop, AJ Kassab and A Minardi. A coupled FDM/BEM solution for the conjugate heat transfer problem. *Numer. Heat Tran. B* 1995; **28**, 139-54.

[8] M He, AJ Kassab, PJ Bishop and A Minardi. An iterative FDM/BEM method for the conjugate heat transfer problem - parallel plate channel with constant outside temperature. *Eng. Anal. Bound. Elem*. 1995; **15**, 43-50.

[9] DA Kontinos. Coupled thermal analysis method with application to metallic thermal protection panels. *J. Thermophys. Heat Tran*. 1997; **11**, 173-81.

[10] CP Rahim, RJ Cavalleri, JG McCarthy and AJ Kassab. Computational code for conjugate heat transfer problems: An experimental validation effort. *In*: Proceedings of the 32nd Thermophysics Conference, Georgia. 1997.

[11] CP Rahim, AJ Kassab and RA Cavalleri. Coupled dual reciprocity boundary element/finite volume method for transient conjugate heat transfer. *J. Thermophys. Heat Tran*. 2000; **14**, 27-38.

[12] Z Xiaoli, S Zhenxu, T Longsheng and Z Gangtie. Coupled flow-thermal-structural analysisof hypersonic aerodynamically heated cylindrical leading edge. *Eng. Appl. Comput. Fluid Mech*. 2011; **5**, 170-9.

[13] L Meng-Sing. A Sequel to AUSM: AUSM+. *J. Comput. Phys*. 1996; **129**, 364-82.

[14] J Blazek. *Computational fluid dynamics: Principles and applications*. Butterworth-Heinemann, Oxford, 2006.

[15] F Pietro and D Domenic. A numerical method for conjugate heat transfer problems in hypersonic flows. *In*: Proceedings of the 40th Thermophysics Conference. Washington. 2008.

[16] HK Veersteeg and W Malalasekera. *An introduction to computational fluid dynamics*. The Finite Volume Method. Pearson, London, 2007, p. 1-503.

[17] K Vinayak, M Viren and KPJ Reddy. Effectiveness of forward facing spike for drag reduction on a large angle blunt cone in hypersonic flow. *J Spacecraft Rockets* 2010; **47**, 542-4.

[18] RK Peetala, D Das, V Kulkarni and N Sahoo. Conjugate heat transfer analysis for a finite thickness cylinder in a hypersonic flow. *Heat Tran. Asian Res*. 2016; **45**, 163-80.

[19] N Sahoo, V Kulkarni and RK Peetala. Conjugate heat transfer study in hypersonic flows. *J. Inst. Eng*. 2018; **99**, 151-8.

[20] RK Peetala, V Kulkarni and N Sahoo. Shock wave boundary layer interactions in hypersonic flows over a double wedge geometry by using conjugate heat transfer. *Heat Tran. Asian Res*. 2021; **50**, 801-17.